Review Article
Open Access
CrossMark

Review on solar thermal power concentrators

Abstract

In this review, an attempt has been made to explore all the possibility of solar thermal concentrator to be used for various applications namely cleaner power generation, heat process, and solar cooking etc. Classification of concentrators, applications, thermal modelling, energy and exergy analysis based on energy balances carried out by many researchers have been reviewed. The optical, thermal and exergy efficiency of some system have also been discussed in terms of concentration ratio. Recent progresses in the advances of solar concentrators integrated with photovoltaic module have been proposed and analyzed with a characteristic equation.

Keywords: solar concentrator, concentration ratio, exergy, photovoltaic thermal

Volume 1 Issue 3 - 2017

Gopal N Tiwari,[1] Deepali Atheaya,[2] Tiwari A,[3]

[1]Bag Energy Research Society (BERS), India
[2]Department of Electrical Engineering, Bennett University, India
[3]Department of Electrical Engineering, Qassim University, Saudi Arabia

Correspondence: Deepali Atheaya, Bennett University, Tech Zone-II, Greater Noida-201310, Uttar Pradesh, India, Tel +91 9910446852, Fax +91 11 26591251, Email datheaya@gmail.com

Received: September 25, 2017 | **Published:** December 29, 2017

Abbreviations: EHC: elliptical hyperboloid concentrator; CR: concentration ratio; CPV: concentrating photovoltaic; FPVC: fresnel lens pv concentrator; ACPPVC: asymmetric compound parabolic photovoltaic concentrator; IASS: inverted absorber solar still; SS: solar still; PVT-CPC: photovoltaic thermal compound parabolic concentrator; DCPC: dielectric photovoltaic thermal compound parabolic concentrator; A_a: aperture area; A_r: receiver of area; HTF: heat transfer fluid; DTIRC: dielectric totally internally reflecting concentrator; TIR: total internal reflection; MSDTIRC: mirror symmetrical dielectric totally internally reflecting concentrator; FHCD: flat high concentration devices; QDs: quantum dots; NPs: nano particles; LR: lumogen f red 300; CSFMSC: curved slats fixed mirror solar concentrator; CLFR: compact linear fresnel reflector; $\dot{m}_f$: mass flow; ΔP: pressure drop; SPLFR: semi-parabolic linear fresnel reflector; PTC: parabolic trough concentrator; PDC: parabolic disk concentrator; HSC: hyperboloid solar concentrator; FLSC: fresnel lens solar concentrator; CPSC: cylindrical parabolic solar concentrator; QDSC: Quantum dot solar concentrator; FMSC: fixed mirror solar concentrator

Introduction

Solar concentrator is a device to operate at high temperature in comparison with conventional flat plate collector. In this case, a beam radiation of solar energy incident over a large surface area is concentrated onto a smaller surface. The concentration is achieved by using a suitable reflecting or refracting elements. This results in an increased solar flux density on the absorber surface and hence gives high temperature in comparison with without concentration. The first largest modern solar furnace, having an operating temperature of 3500°C, was built at Mont Louis, near Odeillo, France in the year 1949 and opened in 1970. It was designed by Professor Félix Trombe. Since then, there were many such furnaces which were built to produce electrical power. The concentrated collectors have potential applications in both thermal and photovoltaic utilization of solar energy at very high delivery temperatures.

Classification of solar concentrators

The classification of solar concentrators can be done on the basis of design, tracking applications and optical properties. These are as follows:

Based on design

In the recent past, there have been a lot of developments in designs of the solar concentrators which are as follows:

a. Parabolic disk concentrator (PDC)
b. Hyperboloid solar concentrator (HSC)
c. Fresnel lens solar concentrator (FLSC)
d. Compound parabolic concentrator (CPC)
e. Cylindrical parabolic solar concentrator (CPSC)
f. Dielectric totally internally reflecting concentrator (DTIRC)
g. Flat high concentration devices (FHCD)
h. Quantum dot solar concentrator (QDSC)
i. Fixed mirror solar concentrator (FMSC)
j. Linear Fresnel reflector
k. Central heliostat tower receiver and
l. Hemispherical bowl mirror etc

Based on optical principle

These are categorized into four groups as follows:

1. **Reflector:** The incident beam radiation on reflector is concentrated to focal point/line. This depends on the design of concentrator. Examples of such reflecting concentrators are parabolic trough, parabolic disk, hyperboloid concentrator and CPC trough etc.

2. **Refractor:** It works on the principle of refractor. In this case, the beam radiation is also refracted either on focal point or line focus. Example of such refracting concentrator is Fresnel lens concentrator.
3. **Hybrid:** In this case, both reflection and refraction takes place to concentrate beam radiation towards focal points. Examples are dielectric totally internally reflecting concentrator (DTIRC) and flat high concentration devices (FHCD).
4. **Luminescent:** The photons of visible wave length of solar radiation will experience total internal reflection and guided towards to solar cell. Example: Quantum Dot Concentrator (QDC).

Based on tracking

There are either tracking or non-tracking concentrators. These are as follows:

a) One axis tracking concentrator: Solar concentrators if rotated along one axis to receive the maximum beam radiation across aperture are known as one axis concentrator such as fixed mirror solar concentrator (FMSC), CPC, linear Fresnel lens reflector/ refractor etc.

b) Two axis tracking concentrator: In this case, two axes tracking of the sun is done to allow both seasonal and daily solar movement, the axes are normally either tip tilt or azimuth altitude. This is done to achieve maximum annual beam radiation with a high concentration ratio for high temperature solar processes. The concentrators with double curvatures are used.

Further, classification can be done on basis of imaging or non-imaging type, line focusing or point focusing and symmetric or asymmetric types of concentrators.

Working principle and review of various concentrators

In this section, working principle and applications of some individual concentrator will be discussed. These are as follows:

Parabolic disk concentrator

If a parabola rotates about its optical axis, it gives the shape of parabolic disk concentration. It is also referred as paraboloidal disk concentrator. The receiver is placed at focal point of parabola with high concentration ratio as shown in Figure 1. Beam radiation falling on inner surface of disk is reflected at focus with finite image. It is a two-axis tracking device. The working fluid in the receiver is heated to high temperatures of about 750-1000°C. The heated fluid is then used to generate electricity by small Stirling Engine or Brayton cycle engine. The engine is attached to the receiver. Parabolic dish systems are the most efficient as compared to the other solar thermal technologies. These types of concentrators are also used for cooking. One such type of solar cooker was installed at Shirdi Sai baba temple Shirdi, Maharashtra, India.[1] This system has been able to cater to the food requirements (3 course meal) of 30,000 people. In this case, the food is cooked with the help of solar energy thus saving a large amount of energy which is drawn from fossil fuels. It causes no harm to the environment and ensures that there is no impact on the global climate. So, we can protect the environment and reduce the climate change which is affecting the planet earth. The concentration ratio (C) with two-way tracking system for point focusing is given by

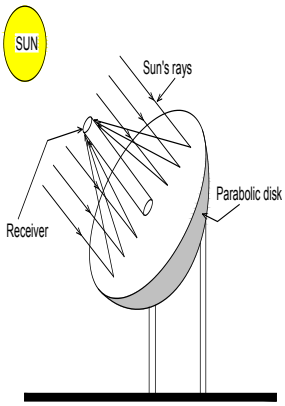

Figure 1 View of parabolic disk concentrator

$$C = \frac{A_a}{A_r} = \frac{1}{\sin^2 \theta_c} \quad \text{..... (1)}$$

Where,

A_a : Aperture Area (m^2)

A_r : Receiver Area (m^2)

θ_c : Half Acceptance Angle

The geometrical concentration ratio for cavity window receiver has been found to be nearly 9000, Li et al.,[2]. The thermal losses in a parabolic disk concentrator are primarily radiative heat losses which can be reduced by decreasing the absorber receiver area. The optimum intercept factor is about 0.95-0.98. The larger must be the absorber size to achieve the optimum beam intercept. The high collection efficiency with a high quality thermal energy is the basic feature of a parabolic disk concentrator operating at very high temperature for power generation. The same design can also be used for pressurized cooking. Following Mawire et al.,[3] the expression for the rate of thermal energy ($\dot{Q}_u$) and exergy output can be written as

$$\dot{Q}_u = \eta_o A_a I_b - U_L A_r \left(T_r - T_a\right) = \eta_o I_b - \frac{U_L}{C}\left(T_r - T_a\right) \quad \text{..... (2)}$$

And

$$\dot{E}x_{out} = \rho_{av} C_{av} \dot{V} \left[\left(T_{fo} - T_{fi}\right) - \left(T_a + 273\right) \ln \frac{T_{fo} + 273}{T_{fi} + 273} \right] \quad \text{..... (3)}$$

Where,

η_0 : Optical Efficiency

A_a : Aperture Area (m^2)

U_L : Heat Loss Coefficient from Receiver to Ambient (W/m^2K)

A_r : Receiver Area (m^2)

The exergy input can be expressed as

$$\dot{E}x_{in} = I_b A_a \left[1 + \frac{1}{3}\left(\frac{T_a + 273}{T_s + 273} \right)^4 - \frac{4\left(T_a + 273\right)}{3\left(T_s + 273\right)} \right] \quad \text{..... (4)}$$

Citation: Tiwari GN, Atheaya D, Tiwari A. Review on solar thermal power concentrators. *MOJ Solar Photoen Sys.* 2017;1(3):71–89.
DOI: 10.15406/mojsp.2017.01.00016

Where,

I_b : Beam Radiation (W/m^2)

T_s : Temperature of Sun

The optical (η_0), thermal (η_{th}) and exergy (η_{ex}) efficiency is defined as follows:

$$\eta_0 = \frac{\dot{Q}_u}{\gamma(\alpha\tau) I_b A_a} \quad \text{..... (5)}$$

$$\eta_{th} = \frac{\dot{Q}_u}{I_b A_a} \quad \text{..... (6)}$$

And

$$\eta_{ex} = \frac{\dot{E}x_{out}}{\dot{E}x_{in}} \quad \text{..... (7)}$$

Where,

η_0 : Optical Efficiency

I_b : Beam Radiation (W/m^2)

A_a : Aperture Area (m^2)

γ : Intercept Factor

α : Absorptivity

n : Number of Tubes

It is important to mention that the optical instantaneous efficiency is always higher than thermal instantaneous efficiency ($\eta_0 > \eta_{th} > \eta_{ex}$). The optical, thermal and energy efficiency of disk concentrator are 52%, 40% and 8 % respectively for cylindrical cavity receiver. Huang et al.,[4] have shown that the optical efficiency of sphere receiver (η_0) varies between 82 to 88%. The intercept factor (γ) in ideal case is 1 without optical error otherwise it is less than 1. The ($\alpha\tau$) is the product of absorptivity of receiver and transitivity of the glazed material. Zanganeh et al.,[5] studied the design of a solar parabolic dish concentrator with polyester membrane facets with small vacuum beneath the membranes. They have used Monte Carlo ray-tracing method and determined the concentration of 8000× at 90% interception factor. Mao et al.,[6] & Li et al.,[7] studied the solar flux and temperature distribution at receiver for the generation of power. Reddy et al.,[8,9] studied the heat loss from receiver and techno-economic viability analysis of 5 MW stand-alone power plants for Indian climatic conditions of solar parabolic dish concentrator. Further, a 500 m^2 paraboloidal dish solar concentrator was designed by Lovegrove et al.,[10] for the generation of power.

Hyperboloid solar concentrator

The shape of hyperboloid solar concentrator can be produced by rotating the two hyperbolic (sections, AB and A_1B_1) design along its symmetrical axis as shown in Figure 2. The diameters of the entrance and exit aperture are referred as D_1 and D_2 and inner surface is reflecting one. The beam radiation incident AA_1 will be reflected back and focused to the exit aperture BB_1. It is a compact hyperboloid solar concentrator and only truncated version of the concentrator is used. For effective application, lenses at the entrance diameter AA_1 are used. Generally, it is mainly used as a secondary concentrator for power production. Saleh et al.,[11] evaluated the optical performance of a static 3-D elliptical hyperboloid concentrator (EHC) by using ray tracing method. It has a concentration ratio (CR) which can be expressed as below

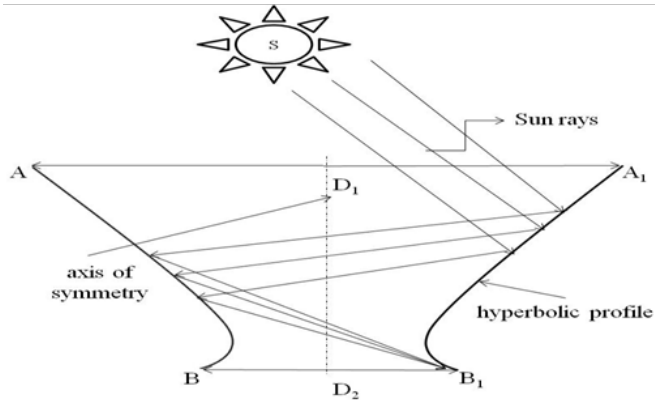

Figure 2 Structure showing a hyperboloid solar concentrator.

CR= 20×, variation of solar incidence angles along receiver major axis

The effective concentration ratio (C_{eff}) is therefore given as:

$$C_{eff} = CR * \eta_0 \quad \text{..... (8)}$$

η_0 : Optical Efficiency

Where, an optical efficiency (η_0) was found to be 27% for concentrator height of 0.4 m and the acceptance angle of ±30°. Imhamed et al.,[12] designed a 3-D elliptical hyperboloid concentrator and experimentally analyzed the system for process heat applications and power generation.

Fresnel lens solar concentrator (FLSC)

A Fresnel lenses solar concentrator (FLSC) consists of one side plane and other side Fresnel lenses. The plane side faces all the parallel beam radiation falling on it and Fresnel lenses side to face photovoltaic cells placed at focal point as shown in Figure 3. It is originally being developed for concentrating photovoltaic (CPV) application for power generation. A linear groove is created on one side of the refracting material. The groove angles are chosen with reference to a particular wavelength of incident beam radiation so that the lens acts as a converging for normal incidence beam radiation. The solar thermal power plant based on linear Fresnel lens reflectors of 125 MW has been installed in Dhursar, India (Table 1). The most preferable material for the construction of Fresnel lenses solar concentrator (FLSC) is plastic which is economical and easy to manufacture. The plastic Fresnel lenses with 20 grooves per mm have been molded. The grooves can also be made for surface facing beam radiation with more reflection losses and more problem of cleaning the top surface. This resulted in low thermal efficiency. There can be either focal point or line focal or flat surface as per requirement. In this case, there is a need to track the sun for maximum beam radiation and hence maximum output. Nishioka et al.,[19] studied the sandblasting durability of acrylic and glass Fresnel lenses for concentrator photovoltaic modules and observed that the durability

of glass Fresnel lens was approximately doubled. The design, analysis of spectrum distribution, optical performance and characterization of Fresnel lenses concentrators has been carried out.[20-23] They have also optimized the design of hybrid Fresnel-based concentrator for generating uniformity irradiance with the broad solar spectrum as shown in Figure 4. Lewandowski et al.,[24] carried out an assessment of linear Fresnel lens concentrators for thermal applications. Xie et al.,[25] reviewed the work carried out on concentrated solar energy thermal applications by using Fresnel lenses.The design of a non-imaging Fresnel lens and reflector solar concentrators have also been studied by Leutz et al.,[26] & Lainé[27]. Chemisana et al.,[28] designed and studied optical performance of a non-imaging linear Fresnel transmissive concentrator for building integration and found that the overall global optical efficiency was 56.38%. The comparative performance of linear Fresnel concentrators for building integrated with and without photovoltaic was done by Chemisana et al.,[29,30] Later on, Wu et al.,[31] conducted an extensive experiment for a point focus Fresnel lens PV Concentrator (FPVC) system. An indoor experiment was performed to investigate a point focus Fresnel lens PV concentrators (FPVC) with a concentration ratio of 100X. It was observed that under natural convection when the ambient temperature (T_a) was 50°C and solar intensity 1000W/m^2, the solar cell efficiency (η_c) decreases to 7.95% and when the T_a was 20°C the η_c was found to be 10%. Zhuang et al.,[32] have considered the following equation for optical axial symmetry.

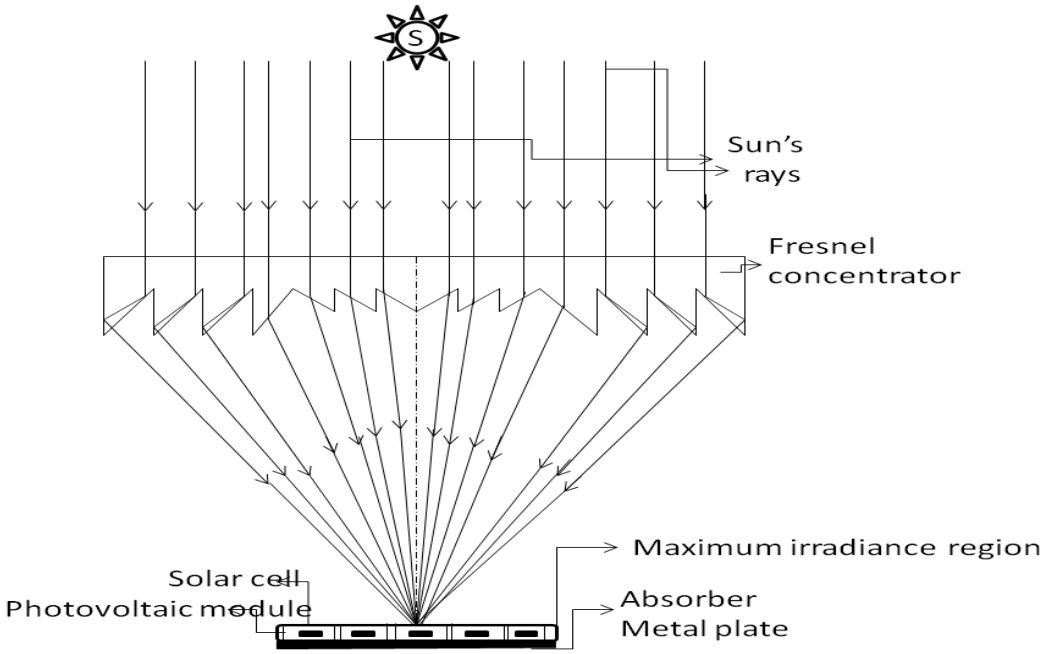

Figure 3 Sketch showing a point focus Fresnel lens concentrator.

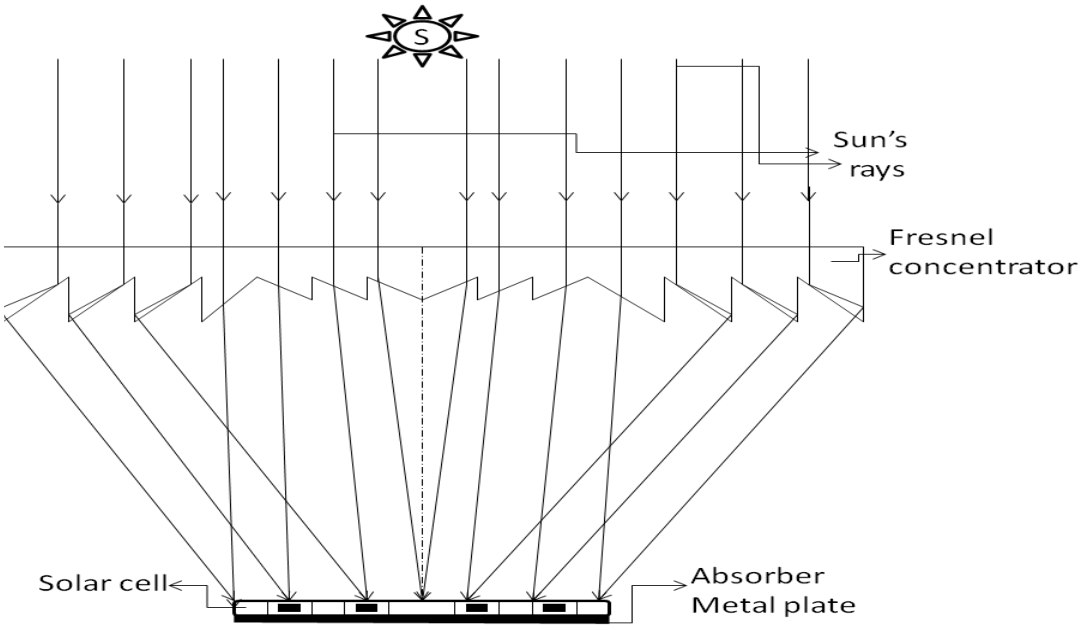

Figure 4 Schematic view of focal plane Fresnel lens concentrator.

Table 1 Some of recent working solar thermal power concentrator plant of capacity 50MW and above all around the world

S. No	Type of Concentrators	Capacity	Manufacturer	Location where Plants have been Installed
1	Central heliostat tower receiver	50MW	Luz	Dagget, California[13]
2	Central heliostat tower receiver	110MW	Abengoa Solar	Chile[14]
3	Central heliostat tower receiver	50MW	SUPCON Solar	Delingha, China[15]
4	Central heliostat tower receiver	37MW	Ivanpah Solar Electric Generating System (ISEGS)	Primm NV, California[15]
5	Central heliostat tower receiver	50MW	Abengoa Solar - IDC	Upington, Northern cape, South Africa[15]
6	Parabolic trough concentrator	50MW	Corporate Ispat Alloys Ltd	Phalodi, Rajasthan, India[16]
7	Linear Fresnel reflector	Two 125 MW power plants	Rajasthan Sun Technique Energy and Reliance Power Ltd.	Dhursar, Rajasthan, India[17]
8	Parabolic trough	100MW	Abengoa Solar - IDC	Poffader, Northern Cape, South[14] Africa
9	Parabolic trough	50MW	Godawari Power Ispat Limited	Nokh, Rajasthan, India[16]
10	Parabolic Trough	50MW	ACS - COBRA group	Talarrubias, Badajoz, Spain[16]
11	Parabolic Trough	50MW	Elecnor/Aries/ABM AMRO	Olivenza, Badajoz, Spain[16]
12	Parabolic Trough	50MW	Megha Engineering and Infrastructure	Megha, Andhra Pradesh, India[16]
13	Parabolic Trough	50MW	Helios II HYPERION Energy Investments, S.L.	Ciudad Real, Puerto Lápice, Spain[16]
14	Parabolic Trough	50MW	FCC Energy	Palma del Río, Córdoba, Spain[16]
15	Parabolic Trough	50MW	FCC Energy	Villena, Alicante, Spain[16]
16	Central heliostat tower receiver	110MW	Crescent Dunes Solar Energy Project (Tonopah)	Tonopah, Nevada, United States[16]
17	Parabolic Trough	250 MW	Genesis Solar, LLC	Blythe, California, United States[18]
18	Parabolic Trough	50MW	Ferrostaal AG	Aldiere, Granada, Spain[16]
19	Parabolic Trough	50MW	Next Era, FPL	Navalvillar de Pela, Badajoz, Spain[16]
20	Parabolic Trough	50MW	Abengoa Solar	Sevilla, Spain[15]
21	Parabolic trough	50MW	RREF/OHL	Morón de la Frontera, Sevilla, Spain[16]
22	Parabolic trough	50MW	Ortiz/TSK/Magtel	Posadas, Córdoba, Spain[16]
23	Parabolic trough	50MW	Elecnor/Aries/ABM AMRO	Alcázar de San Juan, Spain[16]
24	Parabolic trough	50MW	Abengoa Solar - IDC	San José del Valle, Cádiz, Spain[16]
25	Parabolic trough	100MW	Abengoa Solar - IDC	Poffader, Northern Cape, South Africa[16]
26	Parabolic trough	100MW	Iberdrola Renovables Castilla-La Mancha	Puertollano, Castilla-La Mancha, Spain[16]
27	Parabolic trough	100MW	Masdar/Total/Abengoa Solar	Madinat Zayed, 120 km southwest of Abu Dhabi, United Arab Emirates[16]
28	Parabolic trough	50MW	Abengoa (100%)	Logrosán, Cáceres, Spain[16]

Citation: Tiwari GN, Atheaya D, Tiwari A. Review on solar thermal power concentrators. *MOJ Solar Photoen Sys.* 2017;1(3):71–89.
DOI: 10.15406/mojsp.2017.01.00016

$$CR \le \frac{1}{\sin^2 \theta_c} \quad \text{..... (9)}$$

Where θ_c is the half acceptance angle and C is the geometrical CR, defined as

$$C = \frac{A_a}{A_r} \quad \text{..... (10)}$$

Where,

A_a : Aperture Area (m^2)

A_r : Receiver Area (m^2)

Since the apparent angular extent of the sun is ±0.2671°, therefore, the solar concentration limit of the hybrid Fresnel-based concentrator is 46,050 ×, and geometrical CR is about 1759.8× by Eq. (10). Thus, the HCPV system is obtained (CR>300). Larsen et al.,[33] investigated the heat loss in a linear absorber with a trapezoidal cavity of Fresnel reflecting solar concentrator under simulated condition. They observed that heat loss is predominant by radiation of the bottom transparent window due to high operating temperature of for 110°C< T_{pipe} < 285°C. Further, it was reported that heat loss coefficient varied in the range between 3.39 to 6.35 W/m^2 K. After the distribution of solar flux at PV module as shown in Figure 4 the electrical efficiency will increase due to low operating range in comparison to point focus Fresnel lens. Moreover, electrical efficiency can be increased if the back side of PV module is further cooled by flowing of either water/ air (Figure 5) (Figure 6).

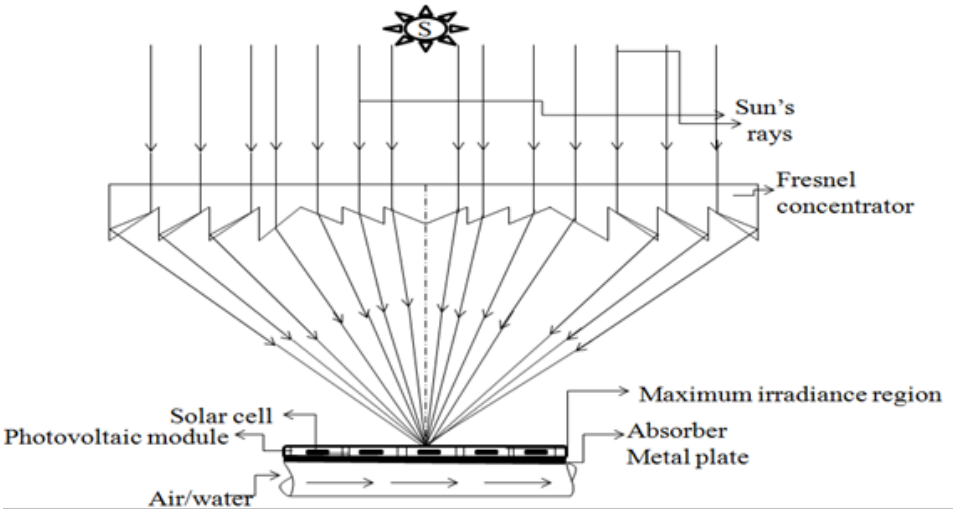

Figure 5 Sketch showing point focus Fresnel lens concentrator with working fluid flowing below the absorber plate.

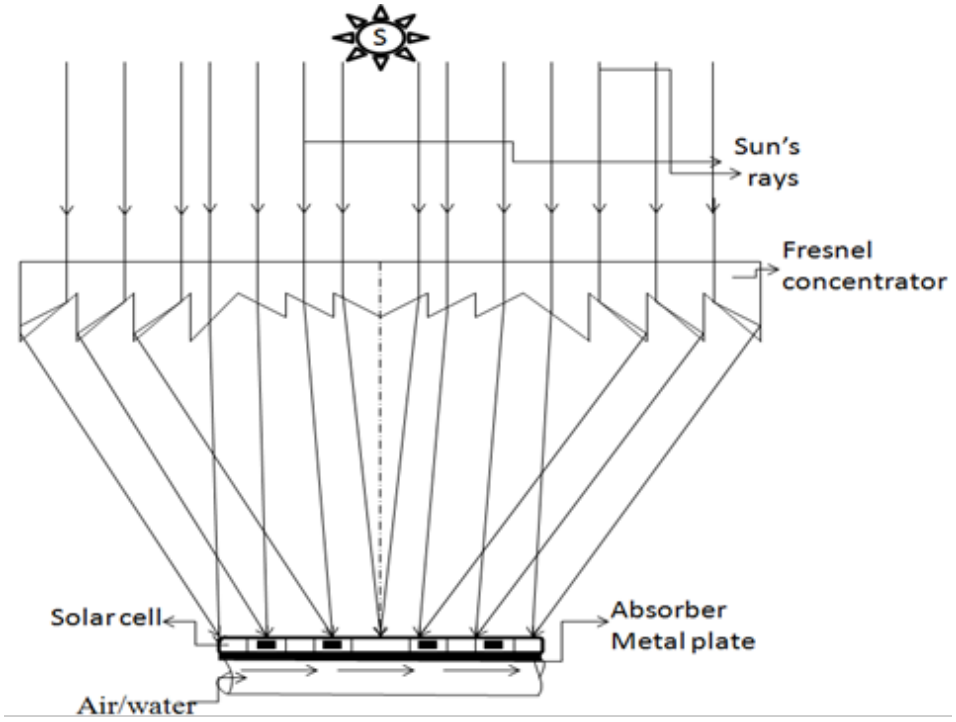

Figure 6 Sketch showing a focal plane Fresnel lens concentrator with working fluid flowing.

Citation: Tiwari GN, Atheaya D, Tiwari A. Review on solar thermal power concentrators. *MOJ Solar Photoen Sys.* 2017;1(3):71–89. DOI: 10.15406/mojsp.2017.01.00016

Compound parabolic concentrator (CPC)

Conventional compound parabolic concentrator (CPC): It consists of rotated parabolic sections which reflect all incident beam radiation to the aperture down to the receiver as shown in Figure 7. This CPC is a non-imaging concentrator with a highest possible concentration ratio (1/sin (θ_a) where θ_a is one-half of the angle permissible by thermodynamic limit for a given acceptance angle, θ_a. Further, it has a large acceptance angle and it needs to be intermittently turned towards the sun. A compound parabolic concentrator (CPC) was initially designed by Winston[34] & Baranov[35] It consists of two parabolic segments which are oriented such that the focus of one is located at the bottom end point of the other one and vice-versa. The axes of the parabolic segments subtend an angle with beam radiation which is equal to acceptance angle. The slope of the reflector surfaces at the aperture plane is parallel to the CPC axis. The receiver is a flat surface parallel to the aperture joining two foci of the reflecting surfaces.

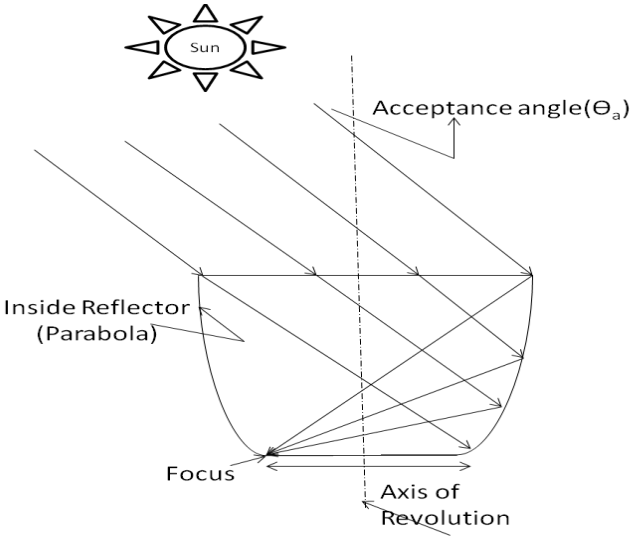

Figure 7 View of a compound parabolic concentrator.

Rabl[36] found that the number of reflections depends on the incident angle, collector depth and concentration ratio. The cost of a unit can be decreased by truncating the CPC to half in height without any significant change in concentration.

$$C = \frac{1}{\sin \theta_c} \qquad \text{..... (11)}$$

Where,

θ_c : Half Acceptance Angle

The compound parabolic concentrator (CPC) is simple in design and modelling and hence has many applications. The thermal performance of a box-type solar cooker integrated with an asymmetric CPC by using Figure 1 & Figure 2 of merit was studied by Harmim et al.,[37] The proposed box type solar cooker remains in a stationary position during its testing which can be integrated into building facade. The design, performance, modelling, experimental validation, heat losses, normal/inverted absorber, asymmetric/symmetric of compound parabolic concentrators for air/water heating systems have been studied by many authors.[38-40]

In order to increase the performance of compound parabolic concentrators (CPC), many parametric studies were carried out by many researchers.[4-46] which includes

a) Fully illuminated inverted V wedge absorbers

b) Reduction of heat losses

c) The minimal reflector surface

d) Air cavity below absorber etc

e) The lowest angular acceptance

f) Minimum number of reflections

Tiba et al.,[47] reported that an annual thermal energy by the CPC, at 80°C is 35% greater than for flat collector with increased reflectivity of the CPC to 0.96 from 55%. Many authors.[48-50] studied the water purification technology by using an inverted absorber solar still (IASS). In this case, solar radiation is reflected back to bottom of solar still by compound either parabolic concentrator or cylindrical reflector. The results were also compared with conventional single slope solar still (SS) by using the concept of characteristic equation. It has been observed that inverted absorber solar still is better. An asymmetric compound parabolic photovoltaic concentrator (ACPPVC) of geometrical concentration ratio 2 was designed and developed by Mallick et al.,[51] which can be used for building facade integration. It was observed that the maximum electrical output power was about 62% more in comparison with non-concentrating collector with 3.4% electrical power and 15% optical losses.

Photovoltaic thermal compound parabolic concentrator (PVT-CPC): A PVT-CPC system is basically consisting of integration of a photovoltaic thermal system and a compound parabolic concentrator system. Guiqiang et al.,[52] & Mallick et al.,[53] studied the electrical and thermal performance of photovoltaic thermal compound parabolic concentrator by using water and air as a working fluid. The hot water/air can be used to heat the room of a building as per requirement. The water and air channel is placed below the PV module at bottom of CPC. They observed that the electrical efficiency of PV module

is increased with an enhanced electrical power. A small dielectric photovoltaic thermal compound parabolic concentrator (dCPC) for the day lighting of the building was developed by Yu et al.,[54] The truncated bottom of dCPC can also be used with PV module to produce electricity. Guiqiang et al.,[55] & Su et al.,[56]proposed a concept of lens-walled compound parabolic concentrator (CPC). They observed that new lens wall CPC has larger half acceptance angle with more uniform flux distribution than mirror CPC with the same geometrical concentration ratio of 4X. The lens-walled CPC has a better annual solar collection performance than the corresponding mirror CPC. Further, Guiqiang et al.,[57] studied the structure of the lens-walled CPC with air gap and found that there is an increase of optical efficiency of 10% due to total internal reflection. Figure 8 illustrates side view of a partially covered photovoltaic thermal compound parabolic concentrator (PVT-CPC). The beam radiation from the sun falls on aperture area (A_a) from where it gets reflected from reflector and descends to the receiver/absorber plate. The receiver of area A_r is half covered with a semitransparent photovoltaic module and the other half is glazed. The water temperature at the outlet of semitransparent PV module covered collector becomes the inlet water temperature of glazed covered flat plate collector. The beam radiation is transferred from the non-packing area of PV module and it gets absorbed by the receiver/absorber plate. Thermal energy from the PV module is transferred to the plate (Figure 9). This leads to an increase in the temperature of absorber plate which further increases the temperature of water. The final outlet temperature from the partially covered PVT-CPC system is. In a PVT-CPC system following cases were analyzed by Atheaya et al.,[58]

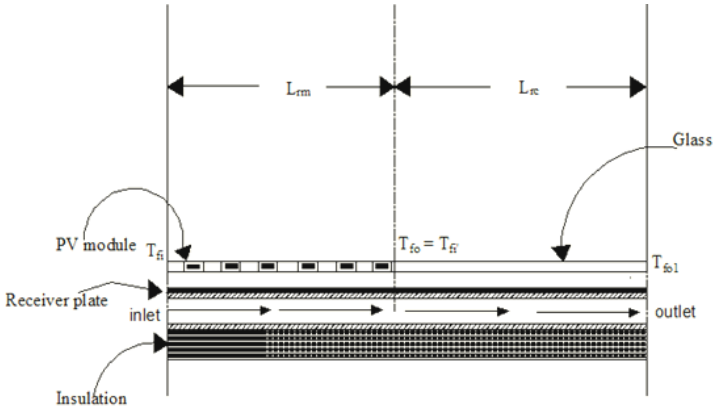

Figure 8 Sectional side view sketch of partially covered PVT-CPC system.

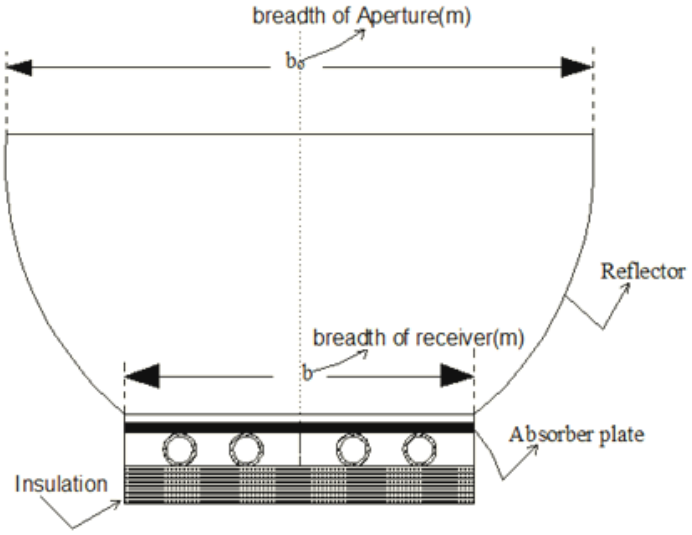

Figure 9 Front view sketch of a partially covered PVT-CPC system.

1) **Case (i)** partially covered PVT-CPC system (The absorber plate is half covered with solar cells and another half is covered with glass).
2) **Case (ii)** fully covered PVT-CPC system (The absorber plate is covered completely by solar cells).
3) **Case (iii)** conventional CPC system (The absorber plate is covered with glass).
4) **Case (iv)** partially covered PVT system (The absorber plate is half covered with solar cells and another half is covered by glass; CPC is absent in this case).

The basic energy balance equation of the PVT-CPC system is as follows:

Lower portion of the PVT-CPC system

For semi-transparent photovoltaic (PV) module

$$\rho\alpha_c\tau_g\beta_c I_c A_{am} = \left[U_{t,ca}\left(T_c - T_a\right) + U_{t,\mathrm{cp}}\left(T_c - T_p\right)\right] A_{rm} + \rho\eta_m I_b A_{am} \quad \ldots\ldots\ldots\ldots\ldots\ldots (12)$$

Citation: Tiwari GN, Atheaya D, Tiwari A. Review on solar thermal power concentrators. *MOJ Solar Photoen Sys.* 2017;1(3):71–89.
DOI: 10.15406/mojsp.2017.01.00016

For blackened tube in plate type absorber

$$\rho\alpha_p\tau_g^2\left(1-\beta_c\right)I_bA_{am}+U_{t,cp}\left(T_c-T_p\right)A_{rm}=F'h_{pf}\left(T_p-T_f\right)A_{rm} \quad \text{..... (13)}$$

For flowing fluid below the absorber

$$\dot{m}_f c_f\frac{dT_f}{dx}dx=F'h_{pf}\left(T_p-T_f\right)bdx \quad \text{..... (14)}$$

Now, the energy balance of conventional CPC collector and flowing fluid can be written as follows:

Absorber

$$\rho\alpha_p\tau_g I_bA_{ac}=F'h_{pf}\left(T_p-T_f\right)bdx+U_{t,pa}\left(T_p-T_a\right)A_{rc} \quad \text{..... (15)}$$

Flowing fluid

$$\dot{m}c_f\frac{dT_f}{dx}dx=F'h_{pf}\left(T_p-T_f\right)bdx \quad \text{..... (16)}$$

Following Tiwari et al.,[59] the rate of thermal energy available from the PVT-CPC water collector is given as

$$\dot{Q}_{u1}=\dot{m}_f\dot{c}_f\left(T_{fo1}-T_{fi}\right)=\left(AF_R\left(\alpha\tau\right)\right)_1I_b-\left(AF_RU_L\right)_1\left(T_{fi}-T_a\right) \quad \text{..... (17)}$$

Where,

$$\left(AF_R\left(\alpha\tau\right)\right)_1=PF_c\left(\alpha\tau\right)_{c,\text{eff}}A_{rc}F_{rc}+PF_2\left(\alpha\tau\right)_{m,eff}A_{rm}F_{rm}\left[1-\frac{A_{rc}F_{rc}U_{l,c}}{\dot{m}_f\dot{c}_f}\right]$$

And

$$\left(AF_RU_L\right)_1=A_{rc}F_{rc}U_{l,c}+A_{rm}F_{rm}U_{l,m}\left[1-\frac{A_{rc}F_{rc}U_{l,c}}{\dot{m}_f\dot{c}_f}\right]$$

An instantaneous thermal efficiency generally known as characteristic equation of PVT-CPC water collector can be obtained as

$$\eta_i=\left(AF_R\left(\alpha\tau\right)\right)_1-\left(AF_RU_L\right)_1\frac{\left(T_{fi}-T_a\right)}{I_a} \quad \text{..... (18)}$$

Where,

ρ : Density

I_b Beam Radiation (W/m^2)

U_L : Heat Loss Coefficient from Receiver to Ambient (W/m^{2}K)

PF_2 : Penalty Factor Due To Absorber/Receiver Plate

PF_c : Penalty Factor Due to Glass Cover for the Portion Covered By Glazing

c_f : Specific heat of fluid (J/kgK)

A_{rm} : Receiver Area Covered by PV Module (m^2)

$\left(\alpha\tau\right)_{eff}$: Product of Effective Absorptivity and Transitivity

The numerical values of $\left(AF_R\left(\alpha\tau\right)\right)_1$ and $\left(AF_RU_L\right)_1$ in Eq. (18) for all cases considered are given in Table 2. The characteristics curve for all the cases are given in Figure 10 & Atheaya et al.,[58] It can be seen from the Figure 10;[58] that the instantaneous thermal efficiency of conventional CPC collector system is maximum because of high thermal gain as compared to other cases. Moreover, the thermal efficiency gain for partially covered PVT-CPC has been less than the partially covered PVT water collector system because of high temperatures. The thermal efficiency gain for fully covered PVT-CPC system was least as compared to all the systems because of high thermal losses.

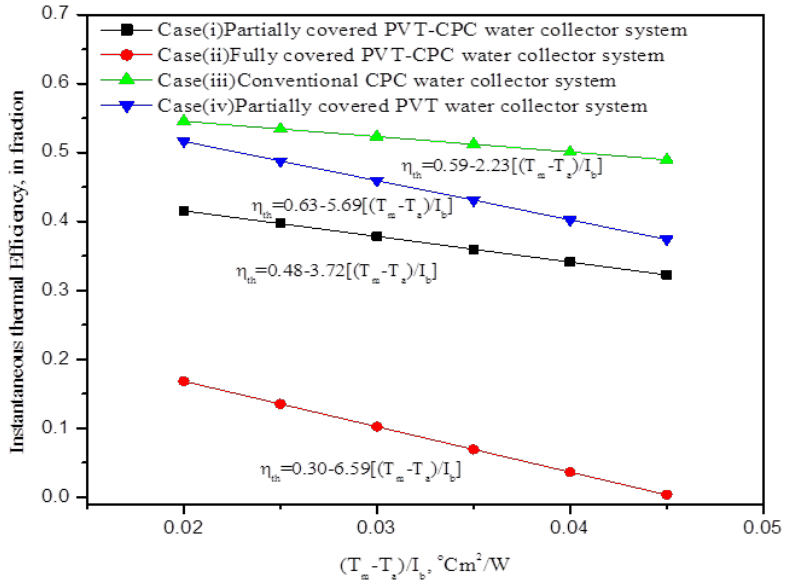

Figure 10 Graph showing a characteristic curve of partially covered PVT-CPC water collector system[Case(i)], fully covered PVT-CPC water collector system[Case(ii)], conventional CPC water collector system[Case (iii)] and partially covered PVT water collector system[Case (iv)].[58]

Citation: Tiwari GN, Atheaya D, Tiwari A. Review on solar thermal power concentrators. *MOJ Solar Photoen Sys.* 2017;1(3):71–89.
DOI: 10.15406/mojsp.2017.01.00016

Table 2 Values of (AFR (ατ)1 and (AFRUL)1 for different cases of PVT-CPC system, Case (i), Case (ii), Case (iii) and case (iv)

Cases	System Description	$\left(AR_F U_L\right)_1$	$\left(AF_R\left(\alpha\tau\right)\right)_1$
Case (i)	Partially covered PVT-CPC system	0.7187	4.6222
Case (ii)	Fully covered PVT –CPC system	0.368	5.4126
Case(iii)	Conventional CPC water collector	0.9848	3.7078
Case (iv)	Partially covered PVT water collector	0.4947	4.2769

Inverted absorber PVT-CPC system: Recently, Atheaya et al.,[60] (Figure 11) have done a comparison study of inverted absorber PVT-CPC system with a normal PVT-CPC system (excluding inverted absorber). They have reported that an IAPVT-CPC system is cost effective.

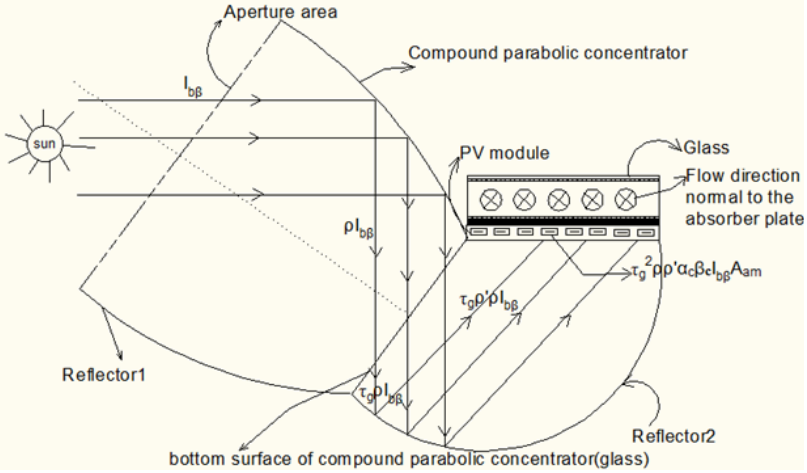

Figure 11 Side view of inverted absorber partially covered PVT-CPC system.[60]

Cylindrical parabolic solar concentrator

A cylindrical parabolic trough concentrator is an optical imaging device. It consists of a cylindrical parabolic reflector with anodized aluminium sheet and a metal tube receiver placed at focal point as shown in Figure 12 & 13, Anon[62] The cylindrical receiver is blackened and glazed with co-axial glass tube which can be rotated about one axis to track the sun's diurnal motion. The heat transfer fluid flows through the receiver for thermal heating. The space between the receiver and glass tube is evacuated to minimize convective heat loss. The concentration ratio for a cylindrical absorber varies from 5 to 30.

$$\eta_i = \frac{\dot{Q}}{I_b A_a} = F_R\eta_o - \frac{F_R A_r}{A_a}U_L\frac{\left(T_{fi}-T_a\right)}{I_b} \quad \ldots\ldots\ldots\ldots\ldots\ldots (19)$$

Where

$$\eta_o = \rho_o\gamma\left(\alpha\tau\right)_{eff}\cos\theta_c \quad \ldots\ldots\ldots\ldots\ldots\ldots (20)$$

Where,

I_b : Beam Radiation (W/m^2)

A_a : Aperture Area (m^2)

A_r : Receiver Area (m^2)

η_0 : Optical Efficiency

F_R : Flow Rate Factor, Dimensionless

U_L : Heat Loss Coefficient from Receiver to Ambient (W/m^{2}K)

ρ_o : Reflectivity

γ : Intercept Factor

$\left(\alpha\tau\right)_{eff}$: Product of Effective Absorptivity and Transitivity

θ_c : Half Acceptance Angle

Ouagued et al.,[63] presented a mathematical model for parabolic trough collector to determine the working fluid temperature, heat gain and heat loss from absorber. The performance has been evaluated for different heat transfer fluid (HTF) for the Algerian climatic condition by them. They noted that heat gain decreases with operating temperature due to more heat losses as expected. The effect of a sphere receiver in the parabolic reflector has been studied by Huan[64] They found that sphere receiver has higher efficiency than solar tower and parabolic trough due to less heat loss and higher cosine factor. Recently, a heat transfer analysis has been carried out by Padilla[65] for a cylindrical absorber of parabolic trough collector. They observed that the heat loss increases with increase of working fluid temperature as expected. Conrado et al.,[66] presented the three dimensional dynamic model for parabolic trough collector with water displacement. List of some of the recent working solar thermal power plants using parabolic trough technology is given in Table 1.

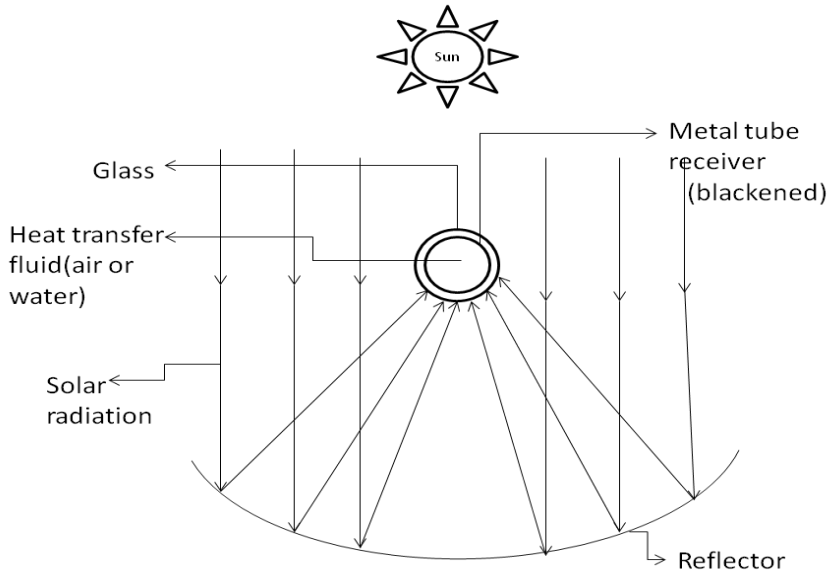

Figure 12 Sketch of a cylindrical parabolic trough concentrator.

Figure 13 Photograph of a cylindrical parabolic trough concentrator.[61]

Dielectric totally internally reflecting concentrator (DTIRC)

Dielectric totally internally reflecting concentrator (DTIRC) works on principle of total internal reflection (TIR) properties of the dielectric medium. A DTIRC consists of three parts namely the front curved surface, the totally internally reflecting sidewall (profile) and the exit aperture. The Figure 14 shows the cross-sectional view of dielectric totally internally reflecting concentrator (DTIRC). In this case, a set of beam radiation incident on the front curved surface at the extreme angle. Each beam radiation is refracted through the front curved surface. Further, it is totally internally reflected from the sidewall (S_1-S_3) and eventually hits the exit aperture (S_3-S_4). In general, the side profile (S_1-S_3) is divided into two parts as:

I. The portion from S_1 to S_2 and

II. The portion from S_2 to S_3.

All beam radiation (extreme rays) between S_1 and S_2 are directed to the corner S_4 after a single total internal reflection (TIR). The beam ray hitting S_2 just satisfies total internal reflection (TIR) and exits from S_4 beam rays between S_2 and S_3, the refractive index is not high enough to totally reflect the extreme rays to S_3.

A mirror symmetrical dielectric totally internally reflecting concentrator (MSDTIRC) integrated PV system was developed by Muhammad et al.,[67,68] Its electrical and optical performances were also investigated for building integrated photovoltaic applications. Their aims were to providing sufficient gain to increase the electrical output of photovoltaic (PV) system and to reduce the size of the PV module for cost effectiveness of system. The MSDTIRC-PV structure is capable of providing a maximum power concentration of 4.2 when compared to a similar PV module without the concentrator.

Citation: Tiwari GN, Atheaya D, Tiwari A. Review on solar thermal power concentrators. *MOJ Solar Photoen Sys.* 2017;1(3):71–89.
DOI: 10.15406/mojsp.2017.01.00016

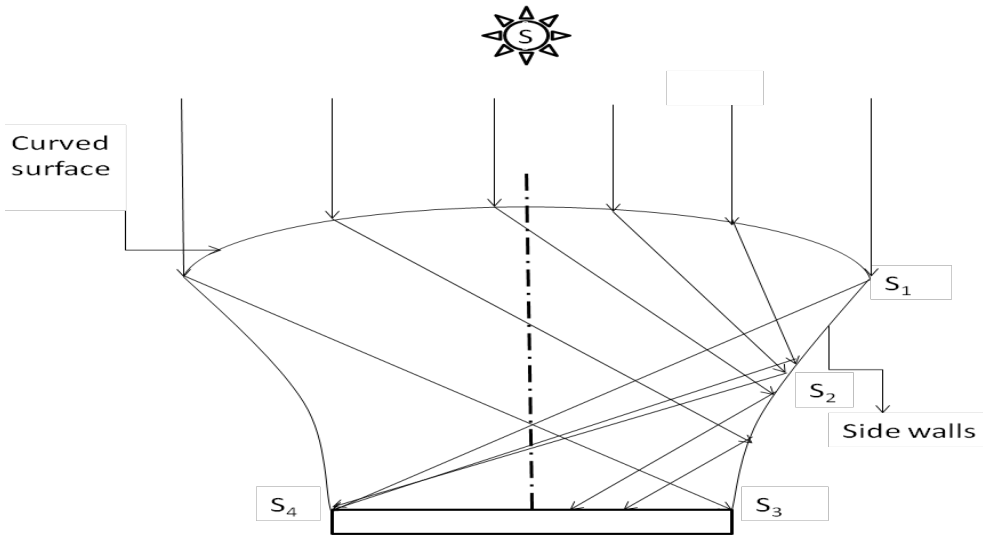

Figure 14 Sketch of a dielectric totally internally reflecting concentrator (DTIRC).

Flat high concentration devices (FHCD), Minano et al.,[69]

In this case, refraction, reflection and total internal reflection take place. The incident beam radiation is first refracted from the top surface and then reflected towards top. After reflection, there is a total internal reflection of beam radiation towards solar cell. There is also a front mirror opposite to the solar cell.

Quantum dot solar concentrator

A quantum dot is a nano crystal. It is made up of semiconductor materials. It is very small and exhibits quantum mechanical properties. The excitations of quantum dots are confined in all three spatial dimensions. The electronic properties of these materials are in between bulk semiconductors and discrete molecules. It increases the efficiency of the solar cell.

The quantum dot solar concentrator has been illustrated in Figure 15. (QDSC) is a novel non-tracking solar concentrator. It consists of three parts namely

a) A transparent sheet of glass/plastic comprising seeded quantum dots (QDs) in materials

b) Reflecting mirrors on three edges/sides and

c) An attached solar cell to exit. In this case, both direct and diffuse solar energy are concentrated on attached photovoltaic cells.

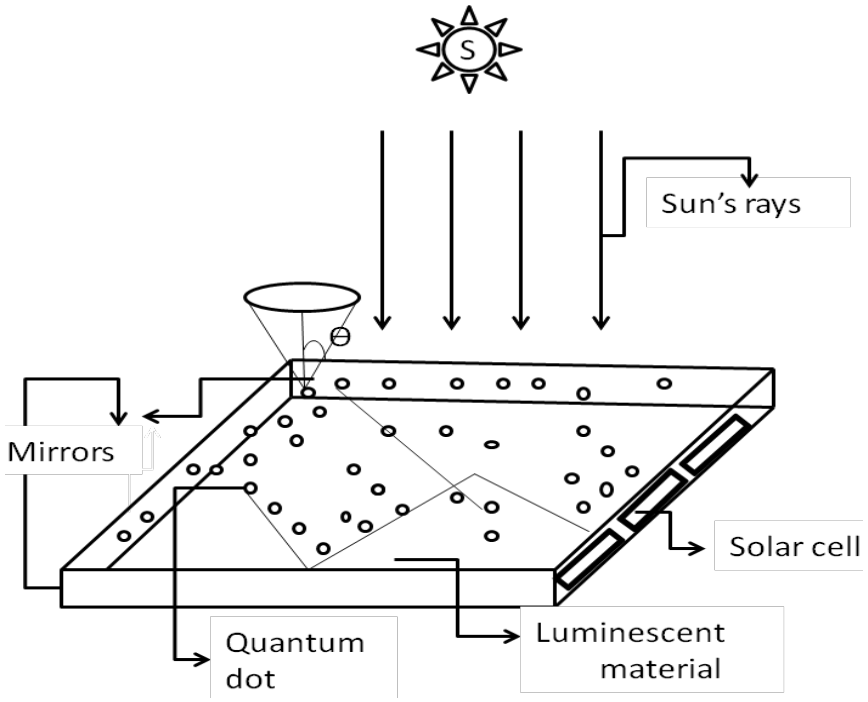

Figure 15 View of a quantum dot concentrator.

The advantages of solar concentrator over conventional flat plate collectors are as follows:

i. It increases the solar intensity at a smaller absorber (receiver) area
ii. The heat-loss area is reduced.
iii. The delivery temperature is very high.
iv. It helps in reducing the cost of absorber/receiver

However, solar concentrator is an optical system and hence the optical losses become important.

Gallagher et al., [70] observed that the system achieved higher concentration factors between 3.78 and 8.65 for polyurethane sample (without QDs) cast in an unmirrored perspex mould. The PV cell was orientated as in a QDSC. The highest fill factor of 0.7 was achieved in a QDSC of 0.08% volume fraction of CdSe/CdS F2 QD. The maximum electrical efficiency was observed to be between 3-3.5%. Chandra et al.,[71] found that the plasmonic excitation enhanced fluorescence of CdSe/ZnS core-shell quantum dots (QDs) in the presence of Au nano particles (NPs) in quantum dot solar concentrator (QDSC) devices. There is a maximum 53% fluorescence emission enhancement for optimum QD/Au NP composite. The electrical conversion efficiency of CdSe core/multishell quantum dots for luminescent solar concentrators found by Bomm et al.,[72] was 2.8% with 45% quantum yields. A concept of quantum dot containing coatings on glass panes for photo luminescent solar concentrators has been proposed by Schüler et al.,[73] It has been recommended that there is a high potential for low-cost fabrication on the large scale and the suitability for architectural integration. Kennedy et al.,[74] reported that there has been an improvement in optical efficiencies and concentration ratios by using near infra-red (NIR) emitting QDs due to the reduction in re-absorption of QD emitted photons can be reduced greatly, thereby diminishing escape cone losses thus. A minimum of 25% escape cone loss can be expected for a plate with refractive index of 1.5 containing QDs with no spectral overlap. Chatten et al.,[75] proposed a novel concentrator with replacement of dye by quantum dots (QDs). Quantum dots (QDs) have advantages over dyes which allows for re-absorption by the QDs. The upper range of efficiency predicted for dye concentrators is around 20%. The performances of luminescent solar concentrators (LSCs) made with quantum dots (QDs) with

(i) CdSe cores,
(ii) ZnS shells and organic dye, Lumogen F Red 300 (LR) were compared by Hyldahl et al.,[76] They observed that the measured fluorescence quantum yield of the CdSe cores QDs (57%) was about half that of LR (>90%) and twice that of ZnS shells QDs (31%).

Fixed mirror solar concentrator (FMSC)

The fixed mirror solar concentrator was introduced firstly by Russell[77] It consists of basically a primary mirror which is kept static and the receiver is moved to track the sun. It is fabricated by using plane mirrors so it is less expensive and the electricity generation is achieved at a much cheaper rate as compared to other solar concentrators. The optical design of a fixed mirror line focused solar concentrator was done by Balasubramanian et al.,[78] by using curved mirror elements. The radius of curvature of curved mirror elements was equal to radius of reference cylinder of concentrator. It was found that the intercept factor is a function of diameter of receiver. The value of intercept factor, γ , is more than 0.9 for diameter of 8cm. Armenta et al,[79] showed that reflectors increased total energy for rows of fixed mirror collectors at no extra footprint. It was also pointed out that appropriate orientation increased total energy but not peak energy collection rate. Kostić et al.,[80] compared the solar thermal collector with and without flat plate reflectors to optimize the optimal position of reflectors. The energy gain of 35-44% was reported in the summer period for optimal position of reflectors which can be an integral part of modern buildings.

Pujol et al.,[81] studied the curved slats fixed mirror solar concentrator (CSFMSC) with a static reflector and a moving receiver as shown in Figure 16 & 17. An optical analysis has been carried out by using ray-tracing tools. The integrated thermal output of the CSFMSC has been determined to evaluate the optimal values for the design parameters at a working fluid temperature of 200°C. They observed that CSFMSC can produce heat at 200°C with an annual maximum thermal efficiency of 51% for the location of Cairo. It can be used for heat process mainly for large scale cooking. The net rate of energy gained for a given an area of aperture (A_a) and receiver area of A_r for CSFMSC is as follows:

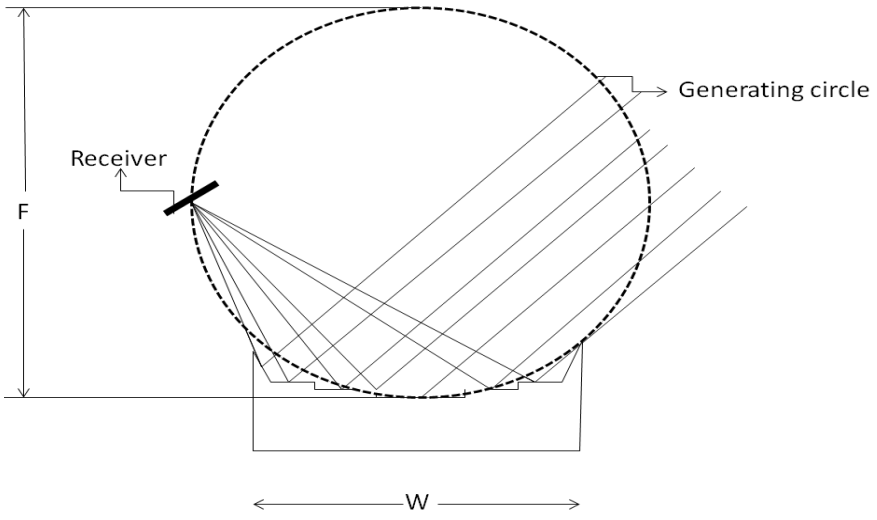

Figure 16 Sketch of the FMSC with focal length and reflector width ratio F/W= 1.5.

Citation: Tiwari GN, Atheaya D, Tiwari A. Review on solar thermal power concentrators. *MOJ Solar Photoen Sys.* 2017;1(3):71–89.
DOI: 10.15406/mojsp.2017.01.00016

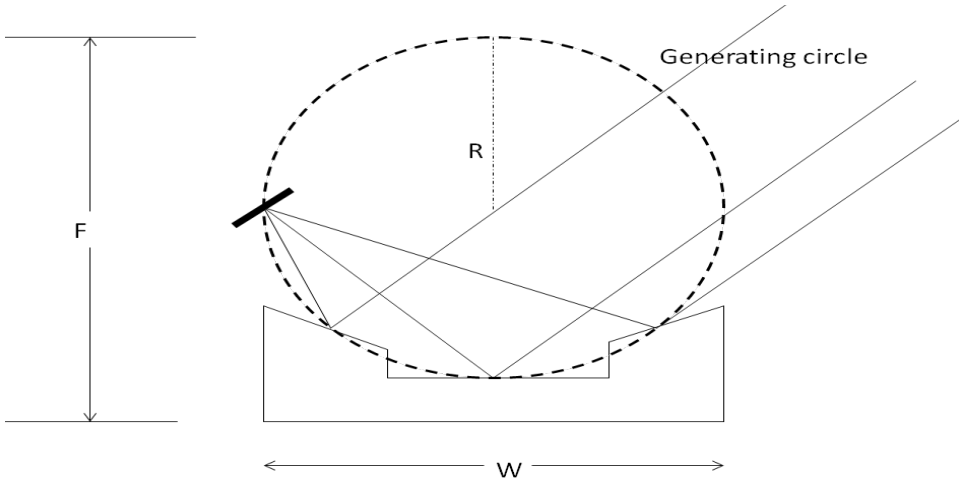

Figure 17 Sketch of the CSFMSC with focal length and reflector width ratio F/W= 1.

$$\dot{Q}_u = F_R\left(\gamma\rho_0\alpha\tau\right) I_{bT} K_{\gamma\rho\alpha\tau} A_a - a_1\left(\overline{T}_w - T_a\right) A_r - a_2\left(\overline{T}_w - T_a\right)^2 A_r \quad \text{..... (21)}$$

or,

$$\frac{\dot{Q}_u}{A_a} = F_R\left(\gamma\rho_0\alpha\tau\right) I_{bT} K_{\gamma\rho\alpha\tau} - \frac{a_1}{C}\left(\overline{T}_w - T_a\right) - \frac{a_2}{C}\left(\overline{T}_w - T_a\right)^2 \quad \text{..... (22)}$$

Where F_R $(\alpha\tau) = 0.859$, $a_1 = 1.214$ W/m^2 K and $a_2 = 0.00435$ W/m^{2}K^2, $\gamma = \rho_o = K_{\gamma\rho\alpha\tau}$ for normal beam radiation.

Linear fresnel reflector

Linear Fresnel reflector is a compact linear Fresnel reflector (CLFR). It is also referred to as a concentrating linear Fresnel reflector. Linear Fresnel reflectors use long, thin segments of mirrors to focus beam radiation onto a fixed inverted flat absorber situated at a common focal point of all reflectors. These reflectors are capable of concentrating the sun's beam radiation to approximately thirty (30) times its normal intensity which gives concentration ratio of 30 as shown in Figure 18. This concentrated solar energy is transferred after absorption to working fluid generally typically oil having boiling temperature very high. The heated fluid (~300^{0}C)) goes to power a steam generator through a heat exchanger. Abbas et al.,[82] presented the steady state thermal behavior of a flat receiver of linear Fresnel concentrator. They have reported that the maximum exergy of LFR at the fluid outlet temperature of 300 °C for a 300 m receiver with 8.33 kW/m^2 impinging radiation at inlet temperature of 200°C was about 30.5%. The maximum thermal efficiency has been reported as 56%. The rate of thermal energy gain (increase in specific enthalpy) of the working fluid flowing with mass

flow rate $\dot{m}_f$ is as follows:

$$\dot{Q}_{gain} = \dot{m}_f c_f \left(T_{f0} - T_{fi}\right) \quad \text{..... (23)}$$

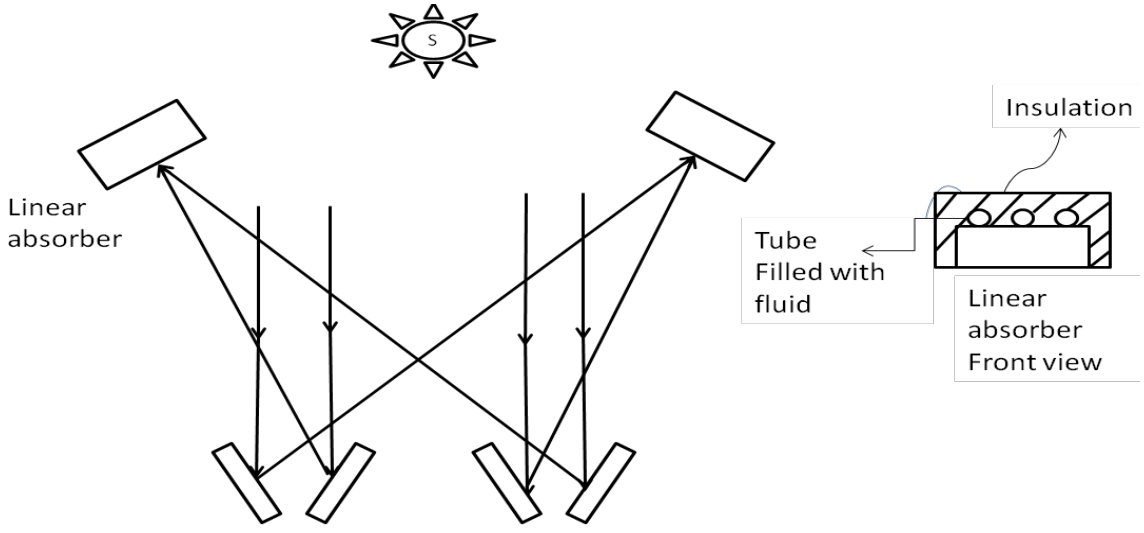

Figure 18 Sketch of a linear Fresnel concentrator.

The T_{f0} and T_{fi} are outlet and inlet temperature of working fluid in receiver. The rate of thermal energy gain through intermediate heat exchanger on basis of heat transfer equation is given by

$$\dot{Q}_{gain} = \varepsilon_f hA\Delta T_{lm} \quad \text{..... (24)}$$

Where ε_f is the geometry factor of an intermediate heat exchanger which can be considered as one due to the similarity between the receiver behavior and an intermediate heat exchanger, A is the heat exchange surface area and ΔT_{lm} is the log mean temperature difference along the receiver. The 'h' is the heat transfer coefficient from the inner surface of the tubes to the working fluid which is can be evaluated, Gnielinski[83] by the correlation as follows:

$$h = \frac{Nu.K}{D} = \frac{f/8(\mathrm{Re}-1000)\mathrm{Pr}}{1+12.5(f/8)^{1/2}\left(\mathrm{Pr}^{2/3}-1\right)} \quad \text{..... (25)}$$

Where Re and Pr are the Reynolds and Prandtl numbers and f is the friction coefficient in tube. The value of h is about 1500 W/m^2°C at 350°C. The value of f varies between 0.0275-0.03 for operating temperature between 200 to 400 °C. It decreases with increase of temperature.

The exergy and thermal efficiency of linear Fresnel reflector (LFR) in a steady state are given by

$$\eta_{ex} = \frac{\dot{Q}_{gain}\left[1-\frac{T_a+273}{T_{f0}+273}\right]-\dot{W}_p}{\dot{Q}_{in}\left[1-\frac{T_a+273}{T_s+273}\right]} \quad \text{..... (26)}$$

And

$$\eta_{th} = \frac{\dot{Q}_{gain}}{\dot{Q}_{in}} \quad \text{..... (27)}$$

The pumping power, $\dot{W}_p$, to overcome the pressure drop associated to the fluid motion in above equation is given by

$$\dot{W}_p = \frac{\dot{m}_f}{\rho}\Delta P \quad \text{..... (28)}$$

The numerical values of $\dot{W}_p$ increases from 0 to 2.25 kW with increase of number tubes in receiver from 10 to 50. An expression for the mass flow ($\dot{m}_f$) and the pressure drop (ΔP) for the hydraulic process characterization are given by

$$\dot{m}_f = \eta\rho\frac{\pi D_i^2}{4}\mu \quad \text{---------- (29)}$$

And

$$\Delta P = f\frac{\rho u^2}{2D_i}2L \quad \text{---------- (30)}$$

Where the factor '2' is given by the fact that the flowing fluid must come back after passing through the receiver.

The convective and radiative heat losses from the inverted trapezoidal cavity receiver for solar linear Fresnel reflector (LFR) has been estimated by using a two dimensional (2-D) numerical model, Reddy et al.,[84] They found that the total heat loss from the inverted trapezoidal cavity receiver varies from 663.47 W/m to 1046.3 W/m for medium temperature (400 °C). It was reported by Sahoo et al.,[85] that radiative component of losses from a trapezoidal cavity was dominant which contributed around 80-90%. This agrees with the result reported by Abbas et al.,[82]; Lin et al.,[86] conducted an experiment and showed that an overall heat loss coefficient of V-shaped cavity receiver in a linear Fresnel reflector (LFR) solar collector varied from 6.25 to 7.52 W/m^2 K for temperature range of 90 to 150°C as per expectation. It was also noted that as the average surface temperature increased from 90 to 150°C, the thermal efficiency decreased from 45% to 37%. A new design of semi-parabolic linear Fresnel reflector (SPLFR) solar concentrator has been proposed by Zhu et al.,[87] The SPLFR is fabricated by linear plate mirrors whose edges located at a parabolic shape line. Based on the ray trace simulation results, it has been observed that the SPLFR has the same concentrating efficiency as that of the parabolic trough concentrator (PTC) with lower manufacturing cost. It is consisted with many linear plate mirrors like linear Fresnel reflector (LFR). To minimize cost per exergy, Nixon et al.,[88] studied a new method for the optimization of the mirror element spacing arrangement and operating temperature of linear Fresnel reflectors (LFR). Their main objectives were to maximize available power output (i.e. exergy) and operational hours. The results showed that the exergy averaged over the year was increased from 9% to 50 W/m^2 with an additional 122 h of operation with cost per exergy of 2.

Central heliostat tower receiver

A heliostat is derived from Helios (the Greek word for sun) and stat (stationary). It is a device which includes a plane mirror which turns to keep reflecting sunlight toward a fixed target shown in Figure 19. This arrangement compensates for the sun's apparent motions in the sky. The fixed target acts as a receiver which is at distant from the heliostat. The reflective surface of the mirror is kept perpendicular to the bisector of the angle between the directions of the sun and the fixed target as seen from the mirror. The fixed target is stationary relative to the heliostat to reflect beam radiation in a fixed direction. The heliostats are normally used for

(i) Day lighting and

(ii) To generate electricity. They can also be sometimes used in solar cooking. Hammache et al.,[89] investigated the thermal efficiency and cost evaluation of high temperature solar heat to produce hydrogen with different levels of yearly direct insolation for various locations at normal incidence from central receiver systems. The study has been carried out with an external vertical cylindrical receiver and for slant sizes ranging from 100 MW to 900 MW. It has been reported that an overall thermal efficiency of the system varies from 51.3 % to 56.1%. The levelized thermal energy cost was in the range of 10 $ GJ for favorable locations. Galal et al.,[90] showed that when the operating temperature was increased from 500 to 1300°C the thermal efficiency of heliostat system decreased from 75% to 55% with down looking cavity type receiver. Further, Collado et al.,[91] made a calculation of the annual thermal energy supplied by a defined heliostat field. A method for the designing of the heliostat field layout has been developed for solar power plant for many researchers [89-95]. Segal et al.,[96] optimized the working temperatures (above 1000K) of solar central receiver to increase its overall efficiency. It was found that when operating temperatures were 1600K and average field density was 35% the maximum

overall efficiency was obtained. Recently, a genetic algorithm was developed by Besarati et al.,[97] to obtain the optimal flux distribution on the receiver surface of a solar power tower plant. Some of the recent working solar thermal power plants based on central heliostat tower receiver technology have been given in Table 1;[94,14-18]

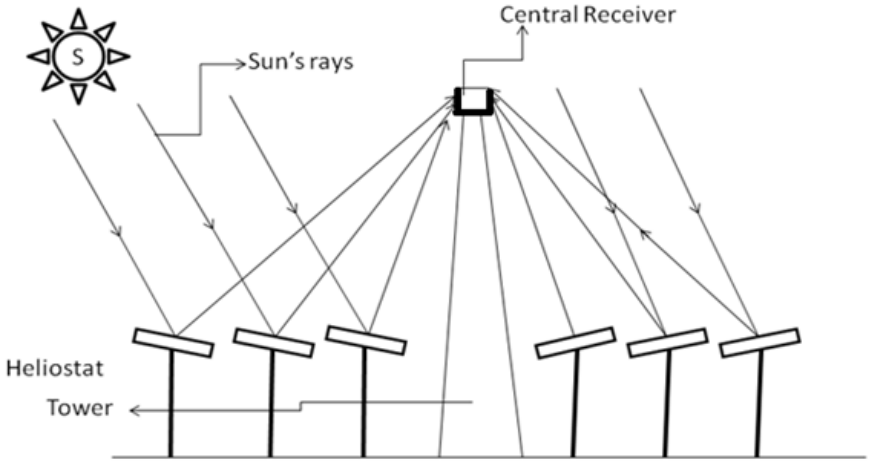

Figure 19 Sketch of a central heliostat tower receiver.

Hemispherical bowl mirror, Tiwari[61]

It consists of a hemispherical mirror as shown in Figure 20.[98] which is always fixed. A tracking linear absorber is also present in it. Here, two-axis tracking is necessary. The absorber is moved so that its axis is always aligned with rays passing through the centre of hemisphere. The linear absorber is pivoted at the centre of curvature of the mirror. The solar rays after reflection enter the hemisphere and cross the paraxial line at some point between the focus and the mirror surface. These designs of concentrator have a lesser concentration because of spherical aberration than the paraboloidal concentrator.

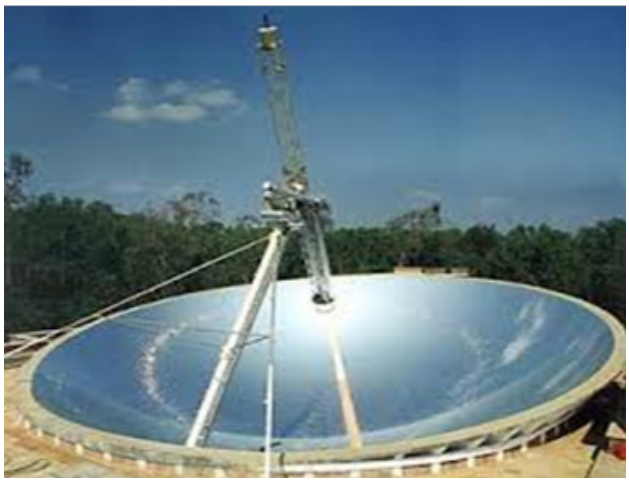

Figure 20 A hemispherical bowl mirror.[98]

Conclusion

Based on the present review on solar power, the following conclusions have been drawn:

1. For low operating temperature say up to 200°C, for example, non-tracking concentrator with small concentration ratio can be used for large scale cooking during peak sunshine hours and space heating for cold climatic conditions.
2. For high operating temperature say about more than 200°C for example power generation (electricity), tracking concentrator with high concentration ratio should be used.
3. For power generation, the constant collection temperature mode is more reliable and preferable.

Recommendations

Following recommendations have been made:

1. For flat absorbing receiver of any concentrating device, the concept of photovoltaic thermal should be analyzed for different configuration for example partially and fully covered PV system.
2. An overall energy and exergy analysis of each solar power system should be carried out.
3. Each solar power generating system should be analyzed from constant flow rate and constant collection temperature mode.
4. Exergoeconomic and Enviroeconomic analysis of each solar power concentrator system should be carried out.
5. Effect of concentration ratio (receiver area) on an overall thermal and exergy of each solar power generating system should be analyzed.

Acknowledgments

We are thankful to the Department of science and Technology and Government of India, New Delhi for partial funding of the research work carried out by us at Indian Institute of Technology, Delhi (India).

Conflicts of interest

The author declares that there is no conflict of interest.

References

1. http://solarcooking.wikia.com/wiki/India
2. Li H, Huang W, Huang F, et al. Optical analysis and optimization of parabolic dish solar concentrator with a cavity receiver. *Solar Energy*. 201392:288–297.

3. Mawire A, Taole SH. Experimental energy and exergy performance of a solar receiver for a domestic parabolic dish concentrator for teaching purposes. *Energy for Sustainable Development*. 2014;19:162–169.
4. Huang W, Huang F, Hu P, Chen Z. Prediction and optimization of the performance of parabolic solar dish concentrator with sphere receiver using analytical function. *Renewable Energy*. 2013;53:18–26.
5. Zanganeh G, Bader R, Pedretti A, et al. A solar dish concentrator based on ellipsoidal polyester membrane facets. *Solar Energy*. 2012;86(1):40-47.
6. Mao Q, Shuai Y, Yuan Y. Study on radiation flux of the receiver with a parabolic solar concentrator system. *Energy Conversion and Management*. 2014;84:1–6.
7. Li Z, Tang D, Du J, et al. Study on the radiation flux and temperature distributions of the concentrator-receiver system in a solar dish/Stirling power facility. *Applied Thermal Engineering*. 2011;31(10):1780–1789.
8. Reddy KS, Kumar NS. An improved model for natural convection heat loss from modified cavity receiver of solar dish concentrator. *Solar Energy*. 2009;83(10):1884–1892.
9. Reddy KS, Veershetty G. Viability analysis of solar parabolic dish stand-alone power plant for Indian conditions. *Applied Energy*. 2013;102:908–922.
10. Lovegrove K, Burgess G, Pye J. A new 500 m^2 paraboloidal dish solar concentrator. *Solar Energy*. 2011;85(4):620-626.
11. Saleh Ali IM, Donovan TSO, Reddy KS, Mallick TK. An optical analysis of a static 3-D solar concentrator. *Solar Energy*. 2013;88: 57–70.
12. Imhamed MSA, Srihari VT, O'Donovan TS, et al. Design and experimental analysis of a static 3-D elliptical hyperboloid concentrator for process heat applications. *Solar Energy*. 2014;102:257–266.
13. Huang W, Li L, Li Y, Han Z. Development and evaluation of several models for precise and fast calculations of shading and blocking in heliostats field. *Solar Energy*. 2013;95:255–264.
14. Tiwari GN. Solar Energy, Fundamentals, design, Modeling and applications. Narosa publishing house, New Delhi, India, 2002. 546 p.
15. www.abengoa.com/web/en/novedades/kaxu/.
16. Behars O, Khellaf A, Mohammedia K. A review of studies on central receiver solar thermal power plants. *Renewable and Sustainable Energy Reviews*. 2013;23:12-39.
17. http://www.nrel.gov
18. http://www.nrel.gov/csp/solarpaces/project_detail.cfm/projectID=272.
19. Nishioka K, Ikematsu K, Ota Y, Araki K. Sandblasting durability of acrylic and glass Fresnel lenses for concentrator photovoltaic modules. *Solar Energy*. 2012;86(10):3021–3025.
20. Yeh N. Optical geometry approach for elliptical Fresnel lens design and chromatic aberration. *Solar Energy Materials and Solar Cells*. 2009;93(8):1309–1317.
21. Yeh N. Analysis of spectrum distribution and optical losses under Fresnel lenses. *Renewable and Sustainable Energy Reviews* 2010;14(9):2926–2935.
22. Chemisana D, Ibáñez M, Rosell JI. Characterization of a photovoltaic-thermal module for Fresnel linear concentrator. *Energy Conversion and Management*. 2011;52(10):3234-3240.
23. Zhuang Z, Yu F. Optimization design of hybrid Fresnel-based concentrator for generating uniformity irradiance with the broad solar spectrum. *Optics & Laser Technology*. 2014;60:27–33.
24. Lewandowski A, Simms D. An assessment of linear Fresnel lens concentrators for thermal applications. *Energy*. 1987;12(2-3): 333-338.
25. Xie WT, Dai YJ, Wang RZ, Sumathy K.Concentrated solar energy applications using Fresnel lenses: A review. *Renewable and Sustainable Energy Reviews*. 2011;15(6):2588-2606.
26. Leutz R, Suzuki A, Akisawa A, Kashiwagi T. Design of a nonimaging Fresnel lens for solar concentrators. *Solar Energy*. 1999;65(6): 379-387.
27. Lainé DC. Transmissive, non-imaging Fresnel types of reflective radiation concentrators revisited. Optics & Laser Technology. 2013;54:274–283.
28. Chemisana D, Rosell JI. Design and optical performance of a non-imaging Fresnel transmissive concentrator for building integration applications. *Energy Conversion and Management*. 2011;52(10):3241-3248.
29. Chemisana D, Ibáñez M. Linear Fresnel concentrators for building integrated applications. *Energy Conversion and Management*. 2011;51(7):1476-1480.
30. Chemisana D, Ibáñez M, Barrau J. Comparison of Fresnel concentrators for building integrated photovoltaics. *Energy Conversion and Management*. 2009;50(4):1079–1084.
31. Wu Y, Eames P, Mallick T, et al. Experimental characterization of a Fresnel lens photovoltaic concentrating system. *Solar Energy*. 2012;86(1):430–440.
32. Zhuang Z, Yu F. Optimization design of hybrid Fresnel-based concentrator for generating uniformity irradiance with the broad solar spectrum. *Optics & Laser Technology*. 2014;60:27–33.
33. Larsen SF, Altamirano M, Hernández A. Heat loss of a trapezoidal cavity absorber for a linear Fresnel reflecting solar concentrator. *Renewable Energy*. 2012;39(1):198–206.
34. Winston R. Principles of solar concentrators of novel design. *Solar Energy*. 1974;16(2):89–95.
35. Baranov VK. Parabolotoroidal mirrors as elements of solar energy concentrators. *Appl Sol Energy*. 1966;2:9–12.
36. Rabl A. Optical and thermal properties of compound parabolic concentrators. Solar Energy. 1976;18(6):497–511.
37. Harmim A, Merzouk M, Boukar M, et al. Performance study of a box-type solar cooker employing an asymmetric compound parabolic concentrator. *Energy*. 2012;47(1):471–480.
38. Harmim A, Merzouk M, Boukar M, et al. Mathematical modeling of a box-type solar cooker employing an asymmetric compound parabolic concentrator. *Solar Energy*. 2012;86(6):1673–1682.
39. Tchinda R. Thermal behavior of solar air heater with compound parabolic concentrator. *Energy Conversion and Management*. 2008; 49(4):529–540.
40. Pramuang S, Exell RHB. Transient test of a solar air heater with a compound parabolic concentrator. *Renewable Energy*. 200530(5):715–728.
41. Kothdiwala AF, Eames PC, Norton B. Optical performance of an asymmetric inverted absorber compound parabolic concentrating solar collector. *Renewable Energy*. 1996;9(1-4):576–579.
42. Kothdiwala AF, Eames PC, Norton B, et al. Technical note: Comparison between inverted absorber asymmetric and symmetric tubular-absorber compound parabolic concentrating solar collectors. *Renewable Energy*. 1999;18(2):277–281.
43. Oommen R, Jayaraman S. Development and performance analysis of compound parabolic solar concentrators with reduced gap losses-oversized reflector. *Energy Conversion and Management*. 2001;42(11):1379–1399.
44. Oommen R, Jayaraman S. Development and performance analysis of compound parabolic solar concentrators with reduced gap losses-'V' groove reflector Renewable Energy. 2002;27(2):259–275.

Citation: Tiwari GN, Atheaya D, Tiwari A. Review on solar thermal power concentrators. *MOJ Solar Photoen Sys*. 2017;1(3):71–89.
DOI: 10.15406/mojsp.2017.01.00016

45. Norton B, Prapas DE, Eames PC, et al. Measured performances of curved inverted-Vee, absorber compound parabolic concentrating solar-energy collectors. *Solar Energy*. 1989;43(5):267–279.

46. Fraidenraich N, Tiba C, Brandão BB, et al. Analytic solutions for the geometric and optical properties of stationary compound parabolic concentrators with fully illuminated inverted V receiver. *Solar Energy*. 2008;82(2):132–143.

47. Tíba C, Fraidenraich N. Optical and thermal optimization of stationary non-evacuated CPC solar concentrator with fully illuminated wedge receivers. *Renewable Energy*. 2011;36(9):2547–2553.

48. Yadav YP, Yadav AK, Anwar N, et al. An asymmetric line-axis compound parabolic concentrating single basin solar still. *Renewable Energy*. 1996;9(1-4):737–740.

49. Dev R, Wahab SAA, Tiwari GN. Performance study of the inverted absorber solar still with water depth and total dissolved solid. *Applied Energy*. 2011;88(1):252-264.

50. Abdul-Wahab SA, Al-Hatmi YY. Performance evaluation of an inverted absorber solar still integrated with a refrigeration cycle and an inverted absorber solar still. *Energy for Sustainable Development*. 2012;17(6):642–648.

51. Mallick TK, Eames PC, Norton B. Power losses in an asymmetric compound parabolic photovoltaic concentrator. Solar Energy Materials and Solar Cells. 2007;91(12): 1137–1146.

52. Guiqiang L, Gang P, Yuehong S, et al. Experiment and simulation study on the flux distribution of lens-walled compound parabolic concentrator compared with mirror compound parabolic concentrator. *Energy*. 2013;58:398–403.

53. Mallick TK, Eames PC, Norton B. Using air flow to alleviate temperature elevation in solar cells within asymmetric compound parabolic concentrators. *Solar Energy*. 2007;81(2):173–184.

54. Yu X, Su Y, Zheng H, et al. A study on use of miniature dielectric compound parabolic concentrator (dCPC) for day lighting control application. *Building and Environment*. 2014;74:75–85.

55. Guiqiang L, Gang P, Yuehong S, et al. Design and investigation of a novel lens-walled compound parabolic concentrator with air gap. *Applied Energy*. 2014;125(15):21–27.

56. Su Y, Riffat SB, Pei G. Comparative study on annual solar energy collection of a novel lens-walled compound parabolic concentrator (lens-walled CPC). *Sustainable Cities and Society*. 2014;4:35–40.

57. Guiqiang L, Gang P, Su Y, et al. Preliminary study based on building-integrated compound parabolic concentrators (CPC) PV/thermal technology. *Energy Procedia*. 2012;14:343–350.

58. Atheaya D, Tiwari A, Tiwari GN, et al. Analytical characteristic equation for partially covered photovoltaic thermal (PVT) compound parabolic concentrator (CPC). *Solar Energy*. 2015;111:176–185.

59. Tiwari GN, Mishra RK, Solanki SC. Photovoltaic modules and their applications: A review on thermal modelling. *Applied Energy*. 2011;88(7):2287–2304.

60. Atheaya D, Tiwari A, Tiwari GN, et al. Performance evaluation of inverted absorber photovoltaic thermal compound parabolic concentrator (PVT-CPC): Constant flow rate mode. *Applied Energy*. 2016;167:70–79.

61. https://en.wikipedia.org/wiki/Genesis_Solar_Energy_Project.

62. http://instamech.blogspot.in/2014/02/who-needs-sunlight-in-arizona-solar.html

63. Ouagued M, Khellaf A, Loukarfi L. Estimation of the temperature, heat gain and heat loss by solar parabolic trough collector under Algerian climate using different thermal oils. *Energy Conversion and Management*. 2013;75:191–201.

64. Huang W, Huang F, Hu P, Chen Z. Prediction and optimization of the performance of parabolic solar dish concentrator with sphere receiver using analytical function. *Renewable Energy*. 2013;53:18–26.

65. Padilla RV, Demirkaya G, Goswami DY, et al. Heat transfer analysis of parabolic trough solar receiver. *Applied Energy*. 2011;88(12): 5097–5110.

66. Conrado LS, Campaña JAM, Montufar CP. Dynamic model of a parabolic trough solar concentrator with a water displacement mechanism. *Renewable Energy*. 2014;63:292–296.

67. Muhammad-Sukki F, Abu-Bakar SH, Ramirez-Iniguez R, et al. Performance analysis of a mirror symmetrical dielectric totally internally reflecting concentrator for building integrated photovoltaic systems. *Applied Energy*. 2013;111:288–299.

68. Muhammad-Sukki F, Siti Hawa AB, Roberto RI, et al. Mirror symmetrical dielectric totally internally reflecting concentrator for building integrated photovoltaic systems. *Applied Energy*. 2014;113:32–40.

69. Minano JC, Gonzalez JC, Zanesco I. Flat high concentration devices Conference record, 24th IEEE PVSC, 1994;1123–1126.

70. Gallagher SJ, Rowan BC, Doran J, et al. Quantum dot solar concentrator: Device optimization using spectroscopic techniques. Solar Energy. 2007;81(4):540–547.

71. Chandra S, Doran J, McCormack SJ, et al. Enhanced quantum dot emission for luminescent solar concentrators using plasmonic interaction. *Solar Energy Materials and Solar Cells*. 2012;98:385–390.

72. Bomm J, Büchtemann A, Chatten AJ, et al. Fabrication and full characterization of state-of-the-art quantum dot luminescent solar concentrators. Solar Energy Materials and Solar Cells. 2011;95(8):2087–2094.

73. Schüler A, Python M, Olmo MV, et al. Quantum dot containing nanocomposite thin films for photo luminescent solar concentrators. *Solar Energy*. 2007;81(9):1159–1165.

74. Kennedy M, McCormack SJ, Doran J, Norton B. Improving the optical efficiency and concentration of a single-plate quantum dot solar concentrator using near infra-red emitting quantum dots. *Solar Energy*. 2009;83(7):978–981.

75. Chatten AJ, Barnham KWJ, Buxton BF, Daukes NJE, Malki MA. A new approach to modelling quantum dot concentrators. *Solar Energy Materials and Solar Cells*. 2003;75(3-4):363–371.

76. Hyldahl MG, Bailey ST, Wittmershaus BP. Photo-stability and performance of CdSe/ZnS quantum dots in luminescent solar concentrators. *Solar Energy*. 2009;83(4):566–573.

77. Russell JL, DePlomb EP, Bansal RK. Principles of the Fixed Mirror Solar Concentrator (2nd edn), General Atomic Co., San Diego, CA, Report No. GA-A 12903, USA, 1974.

78. Balasubramanian V, Sankarasubramanian G. Stretched tape design of fixed mirror solar concentrator with curved mirror elements. *Solar Energy*. 1993;51(2):109–119.

79. Armenta C, Vorobieff P, Mammoli A. Summer off-peak performance enhancement for rows of fixed solar thermal collectors using flat reflective surfaces. *Solar Energy*. 2011;85(9):2041–2052.

80. Kostić LT, Pavlović ZT. Optimal position of flat plate reflectors of solar thermal collector. Energy and Buildings. 2012;45:161–168.

81. Pujol NR, Martínez Moll V. Parametric analysis of the curved slats fixed mirror solar concentrator for medium temperature applications. *Energy Conversion and Management*. 2014;78:676–683.

82. Abbas R, Muñoz J, Val JMM. Steady-state thermal analysis of an innovative receiver for linear Fresnel reflectors. *Applied Energy*. 2012;92: 503–515.

83. Gnielinski V. New equations for heat and mass transfer in turbulent pipe and channel flow. *International chemical engineering*. 1976;16(2):359–368.

84. Reddy KS, Kumar KR. Estimation of convective and radiative heat losses from an inverted trapezoidal cavity receiver of solar linear Fresnel reflector system. *International Journal of Thermal Sciences*. 2014;80:48–57.

85. Sahoo SS, Singh S, Banerjee R. Analysis of heat losses from a trapezoidal cavity used for Linear Fresnel Reflector system. *Solar Energy*. 2012;86(5): 1313–1322.

86. Lin M, Sumathy K, Dai YJ, et al. Experimental and theoretical analysis on a linear Fresnel reflector solar collector prototype with V-shaped cavity receiver. *Applied Thermal Engineering*. 2013;5(1-2):963–972.

87. Zhu J, Huang H. Design and thermal performances of Semi-Parabolic Linear Fresnel Reflector solar concentration collector. *Energy Conversion and Management*. 2014;77:733–737.

88. Nixon JD, Davies PA. Cost-exergy optimization of linear Fresnel reflectors. *Solar Energy*. 2012;86(1):147–156.

89. Hammache A, Bilgen E. Evaluation of thermal efficiency and cost of high temperature solar heat from central receiver systems to use in hydrogen producing thermo chemical processes. *International Journal of Hydrogen Energy*.1988;13(9):539–546.

90. Galal T, Nardin P, Mignot J. An analysis for solar central receiver systems with terminal concentrators or variable apertures. *Solar Energy*. 1988;41(2):147–157.

91. Collado FJ, Turégano JA. Calculation of the annual thermal energy supplied by a defined heliostat field. *Solar Energy.* 1989;42(2):149–165.

92. Wei X, Lu Z, Yu W, et al. A new code for the design and analysis of the heliostat field layout for power tower system. Solar Energy. 2010;84(4):685–690.

93. Pitz-Paal R, Botero NB, Steinfeld A. Heliostat field layout optimization for high-temperature solar thermo chemical processing. *Solar Energy*. 2011;85(2):334–343.

94. Besarati SM, Goswami DY. A computationally efficient method for the design of the heliostat field for solar power tower plant. *Renewable Energy*. 2014;69:226–232.

95. Yao Y, Yeguang H, Shengdong G. Heliostat field layout methodology in central receiver systems based on efficiency-related distribution. *Solar Energy*. 2015;117:114–124.

96. Segal A, Epstein M. Optimized working temperatures of a solar central receiver. *Solar Energy*. 2003;75(6):503–510.

97. Besarati SM, Goswami DY, Stefanakos EK. Optimal heliostat aiming strategy for uniform distribution of heat flux on the receiver of a solar power tower plant. *Energy Conversion and Management*. 2014;84:234–243.

98. http://solarcooking.wikia.com/wiki/File:Solar-cooker-designs-Auroville-bowl_P2.jpg.

Citation: Tiwari GN, Atheaya D, Tiwari A. Review on solar thermal power concentrators. *MOJ Solar Photoen Sys*. 2017;1(3):71–89.
DOI: 10.15406/mojsp.2017.01.00016